The Journal of Clinical Pharmacology
2017, 00(0) 1–10
© 2017, The American College of Clinical Pharmacology
DOI: 10.1002/jcph.1016

Pharmacokinetic Drug Interactions of Apatinib With Rifampin and Itraconazole

Xiaoyun Liu, BS[1,2], Yifan Zhang, PhD[1], Qian Chen, PhD[3], Yan Zhan, PhD[1], Quanren Wang, PhD[4], Chaoying Hu, PhD[3], Chen Yu, BS[3], Zitao Guo, MS[1], Xiaoyan Chen, PhD[1,2], and Dafang Zhong, PhD[1,2]

Abstract

Apatinib is a small-molecule tyrosine kinase inhibitor that has been approved for the treatment of patients with advanced-stage gastric cancer or gastroesophageal junction cancer who have progressed or recurred after at least 2 kinds of systemic chemotherapy. In vitro data indicate that cytochrome P450 (CYP) 3A4 is the primary CYP isoenzyme involved in the metabolism of apatinib. Pharmacokinetic drug–drug interactions of apatinib and (1) a CYP3A4 inducer (rifampin) or (2) a CYP3A inhibitor (itraconazole) were clinically evaluated in healthy volunteers. Compared with the single administration of apatinib, its coadministration with rifampin resulted in a 5.6-fold plasma clearance (CL/F) and 83% decrease in plasma AUC_{0-t} of apatinib. By contrast, coadministration with itraconazole reduced the CL/F of apatinib by 40% and increased its AUC_{0-t} by 75%. In summary, a strong CYP3A4 inducer (rifampin) had a strong effect (>5-fold) on the clinical pharmacokinetics of apatinib, whereas a strong CYP3A inhibitor (itraconazole 100 mg once a day) had a weak effect (1.25- to 2-fold). Whether these effects are of clinical significance needs further research and information about the exposure–safety and exposure–efficacy relationship of apatinib.

Keywords

apatinib, rifampin, itraconazole, drug–drug interaction, pharmacokinetics

Apatinib (YN-968D1) is an oral inhibitor of receptor tyrosine kinases that selectively inhibits vascular endothelial growth factor receptor-2. In 2014, the use of apatinib was approved by the Chinese Food and Drug Administration for the treatment of patients with advanced-stage gastric cancer or gastroesophageal junction cancer who have progressed or recurred after at least 2 kinds of systemic chemotherapy. The clinical efficacy of apatinib was reported in patients with breast cancer, gliomas, and ovarian cancer.[1–3] Apatinib is currently being evaluated in late-stage clinical trials for the treatment of hepatocellular and lung cancers. Apatinib is under development in China, the United States, Europe, and South Korea. On February 27, 2017, orphan designation was granted by the European Commission to Sirius Regulatory Consulting Limited (United Kingdom) for the use of apatinib mesylate in the treatment of gastric cancer.[4]

Based on a population pharmacokinetic (PK) analysis in healthy volunteers and patients with solid tumors, the apparent clearance (CL/F) and apparent volume of apatinib at steady state are predicted to be 57.8 L/h and 112.5 L, respectively. The fractions of the dose in the gut (F1) and central (F2) compartments are 79% and 21%, respectively.[5] In a single-center, nonrandomized, open-label study, patients with advanced colorectal cancer received 28 consecutive days of once-daily administration of 750 mg of apatinib myslate. The average elimination half-life of apatinib was 18.6 hours at steady state. After repeated administration, apatinib had an $AUC_{0-24\,h}$ accumulation ratio of 1.77. Based on the in vitro data, apatinib is highly bound to human plasma protein (92.4%).[6]

Considering that patients with cancer are frequently prescribed multiple medications, whether the coadministration of apatinib with other drugs would result in a drug–drug interaction (DDI) must be determined. This potential DDI could decrease or increase the clearance of apatinib and thus increase or decrease its exposure. Therefore, studies were conducted to identify the clinical relevance of potential DDIs involving CYP-mediated isoenzyme pathways. The systemically available apatinib is extensively metabolized in humans, and the proposed primary

[1]Shanghai Institute of Materia Medica, Chinese Academy of Sciences, Shanghai, China
[2]University of Chinese Academy of Sciences, Beijing, China
[3]Shanghai Xuhui Central Hospital, Shanghai, China
[4]Jiangsu Hengrui Medicine Co. Ltd., Lianyungang, China

Submitted for publication 21 July 2017; accepted 18 August 2017.

Corresponding Author:
Dafang Zhong PhD, 501 Haike Road, Shanghai, China
Email: dfzhong@simm.ac.cn

Xiaoyun Liu, Yifan Zhang, and Qian Chen contributed equally to this article.

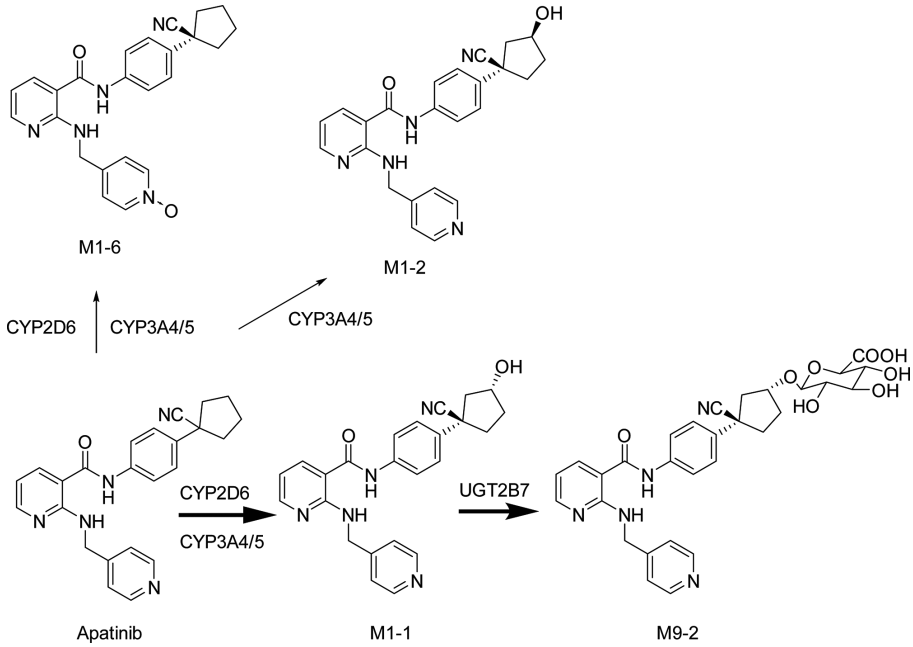

Figure 1. Proposed primary metabolic pathways of apatinib in humans.

metabolic pathway is shown in Figure 1. The primary metabolites are *E*-3-hydroxy-apatinib (M1-1), *Z*-3-hydroxy-apatinib (M1-2), apatinib-25-*N*-oxide (M1-6) and *E*-3-hydroxy-apatinib-*O*-glucuronide (M9-2). The oxidative metabolites of apatinib are formed mainly in the liver. In vitro metabolism studies with recombinant human isozymes and inhibition studies with selective chemical inhibitors of human CYP450 enzymes revealed that the oxidative metabolism of apatinib is mediated by CYP3A4/5 and, to a lesser extent, by CYP2D6, CYP2C9, and CYP2E1.[6] The contributions of CYP3A4, CYP2C9, CYP2E1, and CYP2D6 to the oxidative metabolism of apatinib are 62.6%, 17.0%, 13.1%, and 5.6%, respectively.

In vitro studies reported that apatinib is metabolized primarily by CYP3A4 and an inhibitor of CYP3A4 and CYP2C9. Therefore, the effect of potent CYP3A4 inducers and inhibitors on apatinib PK must be quantified in vivo. Two clinical studies were conducted on healthy volunteers. These studies investigated the PK of a single dose of apatinib administered with and without either rifampin, a potent CYP3A4 inducer (study 1), or itraconazole, a potent CYP3A inhibitor (study 2).

Table 1. Key Inclusion and Exclusion Criteria for Clinical Studies

Inclusion Criteria	Exclusion Criteria
• Aged 18–45 years. • BMI $\geq$ 19 and $\leq$ 24 kg/m^2. • In good health, without heart, liver, kidney, digestive tract, nervous system, and other medical history. • Physical examinations, vital signs, routine laboratory tests, 12-lead electrocardiograms, chest x-ray check normal or abnormal but no clinical significance. • Written informed consent.	• Clinically significant abnormalities in laboratory tests. • Use of any prescription medications or over-the-counter preparations within 14 days. • Intake of alcohol, grapefruit, xanthine, or caffeine within 2 days. • History of surgeries or conditions that could have interfered with or altered GI absorption, distribution, metabolism, or excretion of the study drug. • Infection with human immunodeficiency virus (HIV), hepatitis B, hepatitis C, or syphilis virus. • Had any significant medical condition or gastrointestinal disease, hypertension, or diarrhea. • Drug or alcohol abuse, smoker who consumes more than 10 cigarettes per day. • Pregnant or breastfeeding or woman of reproductive potential not using effective contraception during study and for 3 months following the end of study.

Methods

Clinical Studies

Ethics. Study protocol and informed consent documents were reviewed and approved by the Ethics Committees of Shanghai Xuhui Central Hospital. The design and monitoring of clinical studies complied with the ethical principles of Good Clinical Practice, in accordance with the Declaration of Helsinki. Written informed consent was obtained from the study participants before the initiation of study procedures.

Study Design. Key inclusion and exclusion criteria for the studies are provided in Table 1. Studies 1 and 2 were phase 1, single-center, open-label, 2-treatment,

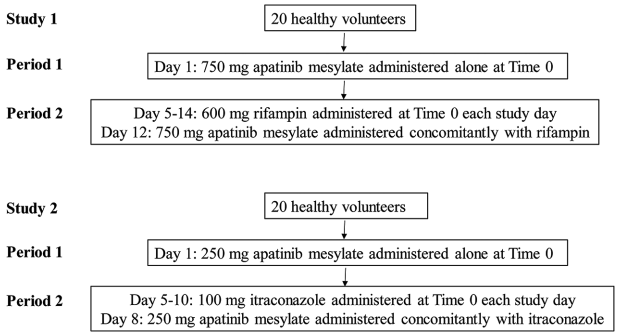

Figure 2. Schematic diagrams of study design.

fixed-sequence DDI studies on healthy volunteers. Study 1 assessed the effect of CYP3A4 induction by rifampin on the single-dose PK of 750 mg of oral apatinib mesylate, whereas study 2 evaluated the influence of CYP3A inhibition by itraconazole on the single-dose PK of 250 mg of oral apatinib mesylate. The design of the 2 studies is shown in Figure 2. A single dose of apatinib alone was administered to subjects during treatment period 1 for both studies. A single dose of apatinib was administered concomitantly with a continuous daily dosage of 600 mg of rifampin (study 1) or 100 mg of itraconazole (study 2) during treatment period 2. Subjects were confined to the study site throughout the study.

All subjects underwent pre- and poststudy medical assessments consisting of physical examinations, routine laboratory tests, vital signs, and 12-lead electrocardiograms. Timing of study drug administration is shown in Figure 2. In both studies, blood samples (3 mL) were collected ≤ 30 minutes before apatinib administration and 0.5, 1.0, 1.5, 2, 3, 4, 6, 8, 12, 24, 48, and 72 hours after dosing for each treatment period for the analysis of apatinib, M1-1, M1-2, M1-6, and M9-2 plasma concentrations.

Analytical Methods. The plasma samples were stored at -70°C and analyzed within the storage stability period. Plasma concentrations of apatinib, M1-1, M1-2, M1-6, and M9-2 were assessed using validated liquid chromatography–tandem mass spectrometry methods. The analysis was conducted on the basis of a published analytical method with modifications as follows. Stable isotope-labeled internal standards were used, the time of analysis was shortened, and the linear range of analytes was changed. Apatinib concentrations were reported as free-base equivalent.[7]

After conducting simple protein precipitation using acetonitrile as the precipitation solvent, all analytes and deuterium internal standards were separated on a Zorbax Eclipse XDB C_{18} column (50 × 4.6 mm, 1.8 μm; Agilent) using acetonitrile: 5 mmol/L ammonium acetate with 0.2% formic acid as the mobile phase with gradient elution. A chromatographic total run time of 5 minutes was achieved. Mass spectrometry detection was conducted through electrospray ionization in positive ion multiple-reaction monitoring mode. The method showed linearity at a concentration range of 2.00–2000 ng/mL for apatinib and M9-2, 1.00–1000 ng/mL for M1-1, and 0.500–500 ng/mL for M1-2 and M1-6. The lower limit of quantification for apatinib, M9-2, M1-1, M1-2, and M1-6 was 2.00, 2.00, 1.00, 0.500, and 0.500 ng/mL, respectively. Assay performance was monitored using quality control samples at apatinib/M9-2/M1-1/M1-2/M1-6 concentrations of 2.00/2.00/1.00/0.500/0.500, 6.00/6.00/3.00/1.50/1.50, 100/100/50.0/25.0/25.0, and 1500/1500/750/375/375 ng/mL for studies 1 and 2. In all concentrations, the coefficient of variation (CV) and accuracy were ≤11.6% and 95%–101% for apatinib, ≤7.9% and 96%–100% for M1-1, ≤9.4% and 96%–99% for M1-2, ≤8.2% and 97%–104% for M1-6, and ≤6.1% and 95%–101% for M9-2, respectively.

Pharmacokinetic Analyses. Pharmacokinetic parameters were calculated by noncompartmental analysis using WinNonlin 6.4 (Pharsight Corp., Mountain View, California). Pharmacokinetic parameters included area under the plasma concentration–time curve from time zero to the time of the last quantifiable concentration (AUC_{0-t}), the AUC from time zero to infinity ($AUC_{0-\infty}$), the maximum observed plasma concentration (C_{max}), the time to maximum observed plasma concentrations (T_{max}), apparent terminal elimination half-life ($t_{1/2z}$), apparent volume of distribution (V_z/F), and apparent clearance (CL/F). The primary PK endpoint measures for the 2 studies were C_{max} and AUC_{0-t}.

Safety Assessments. Tolerability assessments included physical examinations, vital sign measurements (including body temperature, blood pressure, heart rate, breathing rate), 12-lead electrocardiograms, echocardiograms, and laboratory measurements (including hematology, serum chemistry, thyroid function test, and urinalysis). All adverse events (AEs) were recorded and evaluated by investigators in terms of intensity (mild, moderate, or severe), duration, severity, outcome, and relationship to study drug.

Statistical Analyses. For studies 1 and 2, apatinib primary PK end points were analyzed in the presence and absence of rifampin and itraconazole, respectively. Statistical analyses were performed using the log-transformed data of C_{max} and AUC. The magnitude of the DDI was assessed by computing the ratio of the geometric means of the drug in combination versus alone and the corresponding 90% confidence intervals (CIs) based on the log-transformed data. No drug

interaction would be claimed if the 90%CI for the ratio of the geometric mean of the PK parameters fell within 80%–125%. T_{max} differences between the single administration of apatinib and its coadministration with rifampin or itraconazole were examined using a nonparametric test (Wilcoxon signed rank test). A difference was considered significant at $P < .05$.

Results

Clinical Studies

Demographics. Twenty healthy volunteers, including 14 men and 6 women, enrolled in study 1. All subjects completed treatment period 1, whereas 19 (95%) completed treatment period 2. One subject withdrew from the study after the first treatment period (withdrew consent). Mean age was 25.5 years (range, 18–32 years), mean height was 166.4 cm (range, 155.0–178.5 cm), mean body weight was 61.5 kg (range, 48.2–71.4 kg), and mean body mass index was 22.2 kg/m^2 (range, 20.1–23.9 kg/m^2).

Similarly, 20 healthy volunteers, including 16 men and 4 women, enrolled in study 2. All completed treatment periods 1 and 2. Mean age was 25.9 years (range, 20–30 years), mean height was 167.9 cm (range, 154.1–185.9 cm), mean weight was 60.6 kg (range, 49.4–70.3 kg), and mean body mass index was 21.5 kg/m^2 (range, 19.3–23.3 kg/m^2).

Effect of Rifampin on the PK of Apatinib (Study 1). The plasma concentrations and PK parameters for apatinib, M1-1, M1-2, M1-6, and M9-2 are provided in Figure 3 and Table 2, respectively.

C_{max} was achieved at a median T_{max} of 3.0 hours when apatinib was used alone and at a median T_{max} of 2.0 hours in the presence of rifampin. The T_{max} of apatinib did not differ between the single administration of apatinib and its coadministration with rifampin. When coadministered with rifampin, the CL/F of apatinib was 5.6-fold higher than when administering apatinib alone. In addition, the mean $t_{1/2z}$ for apatinib decreased from 11.2 to 5.44 hours following rifampin coadministration.

The 90%CI for the ratio of geometric means (with vs without rifampin) of the C_{max} of apatinib did not fall within the 80%–125% boundary, suggesting that inducing first-pass metabolism by rifampin contributed to decreased plasma concentrations of apatinib. Moreover, the 90%CIs for the ratio of geometric means (with vs without rifampin) of the AUC_{0-t} of apatinib did not fall within the 80%–125% boundary; AUC_{0-t} was reduced by 83%. Combined with the decrease in $t_{1/2z}$, this result suggested that rifampin significantly increased the metabolic clearance of apatinib.

The C_{max} values of M1-6 and M9-2 were increased by 25% and 25%, respectively, whereas those of M1-1 and M1-2 were reduced by 16% and 40%, respectively. The AUC_{0-t} values of M1-1, M1-2, M1-6, and M9-2 were reduced by 78%, 83%, 67%, and 60%, respectively.

Effect of Itraconazole on the PK of Apatinib (Study 2). Plasma concentrations and PK parameters for apatinib, M1-1, M1-2, M1-6, and M9-2 are provided in Figure 4 and Table 3, respectively. C_{max} was achieved at a median T_{max} of 1.5 hours when apatinib was administered with or without itraconazole. The T_{max} of apatinib did not differ between the single administration of apatinib and its coadministration with itraconazole. The CL/F of apatinib coadministered with itraconazole was 40% lower than that when apatinib was given alone. The mean $t_{1/2z}$ for apatinib increased from 7.79 hours to 10.0 hours when coadministered with itraconazole. The 90%CI for the ratio of geometric means (with vs without itraconazole) of the C_{max} of apatinib did not fall within the 80%–125% boundary, suggesting that inhibiting first-pass metabolism by itraconazole contributed to increased plasma concentrations of apatinib. In addition, the 90%CIs for the ratio of geometric means (with vs without itraconazole) of AUC_{0-t} of apatinib did not fall within the 80%–125% boundary, indicating that itraconazole influenced the extent of exposure of apatinib; AUC_{0-t} of apatinib increased by 75% following its coadministration with itraconazole compared with single administration. Combined with the increase in $t_{1/2z}$, these results suggested that itraconazole decreased the metabolic clearance of apatinib.

The C_{max} values of M1-1 and M9-2 were reduced by 10% and 2.5%, respectively, whereas those of M1-2 and M1-6 were increased by 42% and 12%, respectively. The AUC_{0-t} values of M1-1, M1-2, M1-6, and M9-2 were increased by 58%, 111%, 46%, and 28%, respectively.

Safety Summary. Overall, no deaths or serious AEs were reported throughout the study. All treatment-related AEs were of mild intensity and did not require dose adjustment or medical treatment. None of the subjects withdrew because of AEs. In study 1, urine discoloration was reported in all subjects during treatment with rifampin and disappeared after discontinuation of rifampin. Other treatment-related AEs, reported in 5 subjects (25.0%), included nausea, vomiting, bitter taste, and increased blood bilirubin. Only increased blood bilirubin occurred during treatment with apatinib alone; other treatment-related AEs occurred during treatment with rifampin alone. Five subjects (25.0%) reported 1 or more treatment-related AEs during study 2, including increased serum bilirubin, increased alanine aminotransferase, hyperuricemia, hypertriglyceridemia, and oral mucositis. Only 1 oral

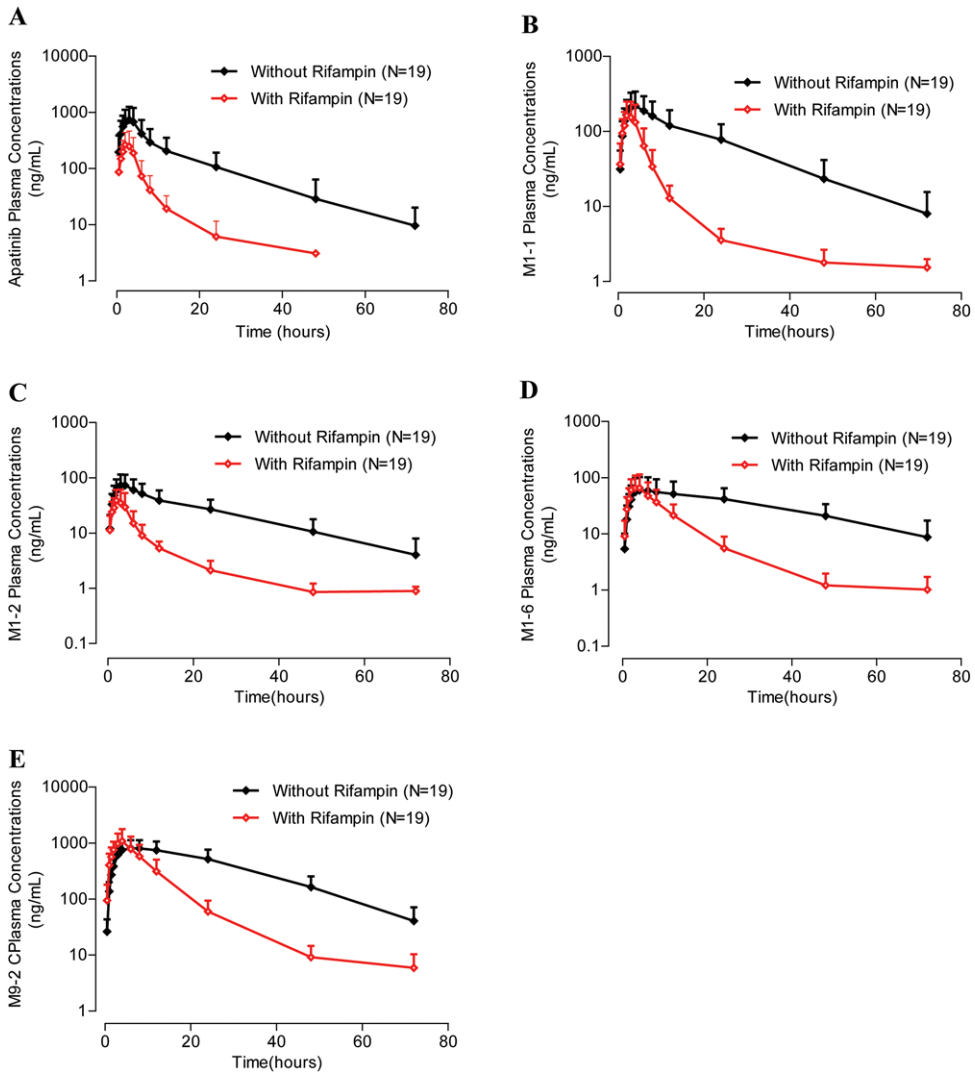

Figure 3. Mean (SD) plasma concentration–time profiles of (A) apatinib, (B) M1-1, (C) M1-2, (D) M1-6, and (E) M9-2 following administration of 750 mg apatinib mesylate with or without rifampin in healthy adults. Semilogarithmic axes.

mucositis occurred during treatment with itraconazole alone; other treatment-related AEs occurred during treatment with apatinib alone or with apatinib plus itraconazole.

Discussion

The metabolism of apatinib in humans exhibits stereoselectivity. Apatinib was primarily catalyzed by CYP3A4 and CYP3A5 to form M1-2, and a small amount of M1-1 was produced by the catalysis of CYP2D6, CYP3A4, and CYP3A5. During the catalysis of alcohol dehydrogenase, M1-1 and M1-2 can form the dehydrogenation product M5-4, and the reaction rate of M1-1 is faster than M1-2. M5-4 can be further reduced to M1-1 and M1-2 under aldehyde–ketone reductase and tends to generate additional M1-1, resulting in the higher system exposure of M1-1 than of M1-2. UDP-glucuronosyltransferase (UGT) 2B7 catalyzes M1-1 to form substantial *O*-glucuronide conjugates (M9-2), whereas UGT1A4 and UGT2B7 catalyze M1-2 to form small amounts of *O*-glucuronide conjugates (M9-1). In vitro studies indicated that CYP3A4 is the main enzyme involved in the metabolism of apatinib to M1-2.[6] Therefore, the PK drug interactions of apatinib during coadministration with a CYP3A4 inducer (rifampin) and a CYP3A inhibitor (itraconazole) were investigated in 2 separate clinical studies.

Determining the steady-state PK of apatinib in the absence and presence of CYP3A4 inducers or inhibitors is the preferred methodology to assess PK drug interactions in these studies. This study design is not appropriate for cancer patients because of the potential to reduce or increase the exposure to apatinib, thereby leading to decreased efficacy or increased toxicity, respectively. Apatinib has an acceptable tolerability

Table 2. Pharmacokinetic Parameters and Statistical Analyses of Apatinib, M1-1, M1-2, M1-6, and M9-2 Following Administration of 750 mg Apatinib Mesylate Without or With Rifampin

			Apatinib Mesylate 750 mg			
Analyte	Parameter	Summary Statistic	Alone (n = 19)	+ Rifampin (n = 19)	Ratio (%)	90%CI of Ratio
Apatinib	C_{max}, ng/mL	Gmean (CV%)	681 (62.2)	265 (64.4)	39.0	32.2–47.1
	AUC_{0-t}, μg·h/mL	Gmean (CV%)	6.86 (76.1)	1.16 (74.7)	16.9	14.0–20.5
	$AUC_{0-\infty}$, μg·h/mL	Gmean (CV%)	7.15 (74.7)	1.22 (72.1)	17.0	14.2–20.4
	T_{max}, h	Median (range)	3.00 (1.00-4.00)	2.00 (1.00-4.00)		
	$t_{1/2z}$, h	Mean (SD)	11.2 (3.8)	5.44 (1.56)		
	V_z/F, L	Mean (SD)	2220 (2100)	5680 (4170)		
	CL/F, L/h	Mean (SD)	130 (92)	726 (478)		
M1-1	C_{max}, ng/mL	Gmean (CV%)	197 (53.8)	166 (48.9)	84.2	73.6–96.5
	AUC_{0-t}, μg·h/mL	Gmean (CV%)	4.07 (57.4)	0.874 (54.3)	21.5	18.7–24.6
	$AUC_{0-\infty}$, μg·h/mL	Gmean (CV%)	4.30 (56.3)	0.908 (52.6)	21.1	18.3–24.3
	T_{max}, h	Median (range)	4.00 (1.00-6.00)	2.00 (1.00-4.00)		
	$t_{1/2z}$, h	Mean (SD)	15.1 (10.3)	8.79 (7.97)		
M1-2	C_{max}, ng/mL	Gmean (CV%)	66.2 (54.2)	39.4 (53.5)	59.6	52.2–68.0
	AUC_{0-t}, μg·h/mL	Gmean (CV%)	1.45 (50.6)	0.248 (52.3)	17.1	14.7–20.0
	$AUC_{0-\infty}$, μg·h/mL	Gmean (CV%)	1.58 (50.7)	0.274 (48.1)	17.3	15.0–20.0
	T_{max}, h	Median (range)	3.00 (1.50-4.00)	2.00 (1.00-4.00)		
	$t_{1/2z}$, h	Mean (SD)	18.7 (12.2)	11.9 (8.5)		
M1-6	C_{ma-x}, ng/mL	GMean (CV%)	50.1 (69.9)	62.8 (63.3)	125.3	106.3–147.7
	AUC_{0-t}, μg·h/mL	GMean (CV%)	1.94 (60.5)	0.637 (60.0)	32.8	28.0–38.4
	$AUC_{0-\infty}$, μg·h/mL	GMean (CV%)	2.36 (61.9)[a]	0.673 (56.4)	29.3[a]	24.5–35.1
	T_{max}, h	Median (range)	6.00 (3.00-24.0)	3.00 (1.00-4.00)		
	$t_{1/2z}$, h	Mean (SD)	23.9 (13.8)[a]	9.30 (6.53)		
M9-2	C_{max}, ng/mL	GMean (CV%)	781 (40.7)	973 (60.8)	124.6	107.9–143.9
	AUC_{0-t}, μg·h/mL	GMean (CV%)	23.7 (42.9)	9.54 (55.2)	40.2	34.6–46.6
	$AUC_{0-\infty}$, μg·h/mL	GMean (CV%)	24.7 (42.2)	9.69 (54.2)	39.2	33.8–45.6
	T_{max}, h	Median (range)	6.00 (4.00-12.0)	4.00 (1.50-4.00)		
	$t_{1/2z}$, h	Mean (SD)	13.6 (6.0)	8.45 (6.29)		

C_{max}, maximum observed concentration; AUC_{0-t}, area under the concentration–time curve from time zero to the last measurable concentration point; $AUC_{0-\infty}$, area under the concentration–time curve from time zero to infinity; T_{max}, time of the maximum concentration; $t_{1/2z}$, apparent terminal elimination half-life; V_z/F, apparent volume of distribution; CL/F, apparent clearance; GMean, geometric mean; CV, coefficient of variation; mean, arithmetic mean; SD, standard deviation; CI, confidence interval.

[a]Only 18 healthy volunteers had evaluable area under the concentration–time from zero to infinity and apparent terminal elimination half-life.

profile that permits single doses (750 mg) to be administered to healthy volunteers without the significant risk of adverse reactions; however, multiple doses at therapeutic levels may result in unacceptable adverse effects in this population. Therefore, these studies were conducted in healthy volunteers using single doses of apatinib with or without steady-state levels of rifampin and itraconazole.

Rifampin induces several drug-metabolizing enzymes, including CYP1A2, CYP2A6, CYP2B6, CYP2C9, CYP3A4, UGTs, glutathione-S-transferases, and aldehyde dehydrogenase, and some drug transporters, such as P-glycoprotein (P-gp), multidrug resistance protein 2, and organic anion-transporting polypeptide 2.[8,9] A dose of 600 mg once-daily rifampin is recommended by the US Food and Drug Administration Guidance for Industry in evaluating the potential drug interactions that involve CYP3A4 induction.[10]

A rifampin dose at 600 mg once daily significantly reduces the exposure for other tyrosine kinase inhibitors such as imatinib, nilotinib, dasatinib, gefitinib, and erlotinib, which are CYP3A4 substrates.[11–15]

A daily administration of rifampin (600 mg) can induce maximum CYP3A4 induction on day 7.[16] In study 1, rifampin was administered for 7 days, and then continued for an additional 3 days to maintain the maximal levels of induction during the 3-day apatinib PK sampling in treatment period 2.

The geometric mean values of apatinib C_{max} and AUC_{0-t} were markedly reduced during coadministration with rifampin compared with those during single doses administered alone; the result is nonequivalent. The $t_{1/2z}$ value was also reduced in the presence of rifampin. A reduced level of apatinib exposure combined with a shorter $t_{1/2z}$ is indicative of an increase in first-pass metabolism, systemic clearance, or both because of the induction of CYP3A4 by rifampin.

However, the AUC_{0-t} values of M1-1, M1-2, M1-6, and M9-2 were markedly reduced. The C_{max} values of M1-1 and M1-2 were reduced by 16% and 40%, respectively, whereas those of M1-6 and M9-2 were increased

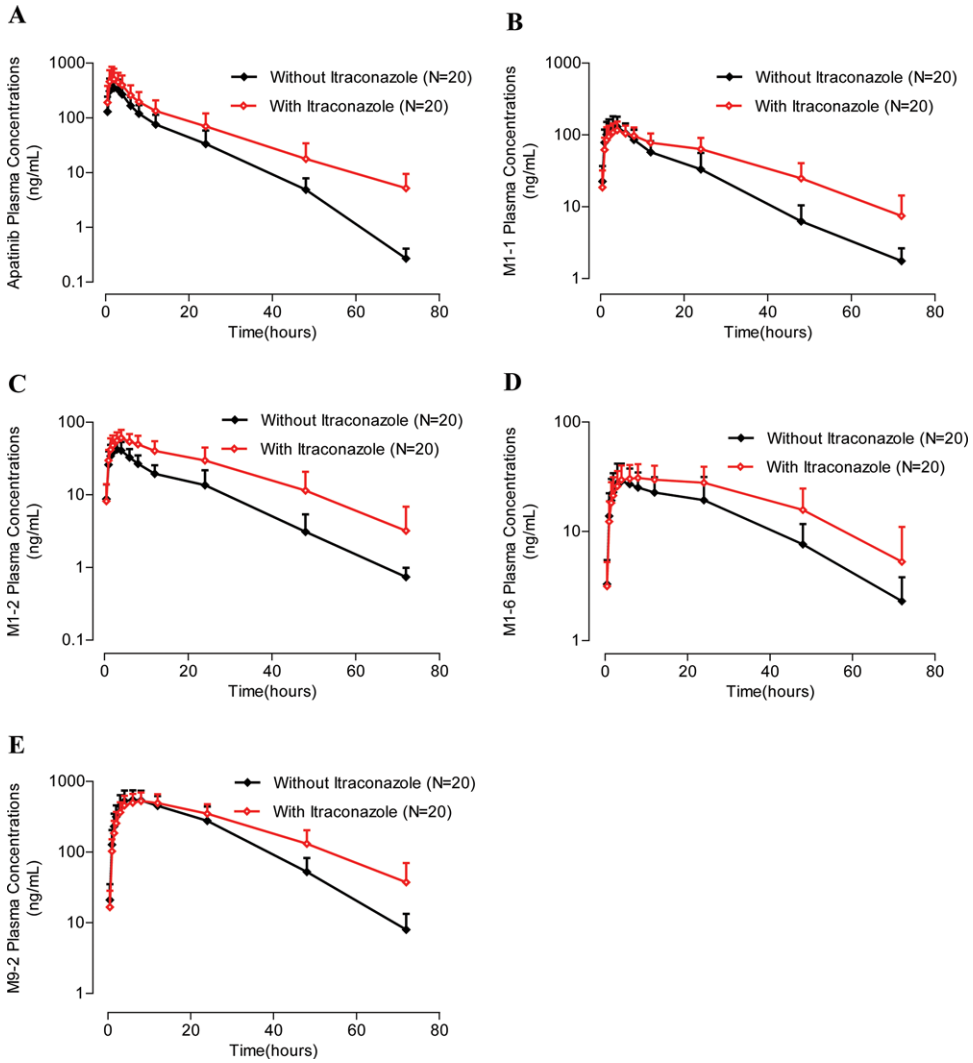

Figure 4. Mean (SD) plasma concentration–time profiles of (A) apatinib, (B) M1-1, (C) M1-2, (D) M1-6, and (E) M9-2 following administration of 250 mg apatinib mesylate with or without itraconazole in healthy adults. Semilogarithmic axes.

by 25%. The $t_{1/2z}$ of M1-1, M1-2, M1-6, and M9-2 was also reduced in the presence of rifampin, which indicates that rifampin also induces the metabolism and excretion of M1-1, M1-2, M1-6, and M9-2. In vitro studies indicated that M1-1, M1-2, and M1-6 can be further metabolized by CYP3A4 (unpublished data). When accounting for differences in molecular weight, the ratio of geometric mean AUC_{0-t} between M1-1 and M1-2 increased from 2.81 to 3.52 following coadministration. Rifampin can induce UGT2B7 activity. When accounting for differences in molecular weight, the ratio of the geometric mean AUC_{0-t} between M9-2 and M1-1 increased from 4.08 to 7.65 following coadministration. In vitro studies revealed that M1-1, M1-2, and M1-6 are P-gp and breast cancer resistance protein (BCRP) substrates (unpublished data). Rifampin may induce P-gp-mediated excretion, thereby reducing the AUC_{0-t} and $t_{1/2z}$ of M1-1, M1-2, and M1-6. Given that M9-2 is the *O*-glucuronide conjugate of M1-1, the exposures of M1-1 and M9-2 were reduced accordingly.

Itraconazole is a potent inhibitor of CYP3A. Five repeated administrations of 200 mg of itraconazole have been shown to increase the plasma exposure of domperidone by 3.2-fold.[17] Four repeated administrations of 200 mg of itraconazole increased the plasma exposure of atorvastatin acid, atorvastatin lactone, and felodipine about 3-, 4-, and 6-fold, respectively.[18,19] Ke et al identified itraconazole (200 mg twice daily on day 1, once daily on days 2–6) as acceptable ketoconazole alternatives.[20] The Clinical Pharmacology Leadership Group recommends an itraconazole dosing regimen of 200 mg once daily with a 3-day run-in period prior to its coadministration with the substrate. After the day of substrate coadministration (day 4), itraconazole dosage must constantly cover 4 to 5 half-lives of the substrate.[21] In study 2, 100 mg of itraconazole was

Table 3. Pharmacokinetic Parameters and Statistical Analyses of Apatinib, M1-1, M1-2, M1-6, and M9-2 Following Administration of 250 mg Apatinib Mesylate Without or With Itraconazole

			Apatinib Mesylate 250 mg			
Analyte	Parameter	Summary Statistic	Alone (n = 20)	+ Itraconazole (n = 20)	Ratio (%)	90%CI of Ratio
Apatinib	C_{max}, ng/mL	GMean (CV%)	371 (44.1)	496 (53.8)	133.7	103.9–171.9
	AUC_{0-t}, μg·h/mL	GMean (CV%)	2.80 (49.7)	4.88 (57.0)	174.5	135.7–224.3
	$AUC_{0-\infty}$, μg·h/mL	GMean (CV%)	2.94 (50.0)	5.02 (56.1)	170.5	134.3–216.5
	T_{max}, h	Median (range)	1.50 (1.00–3.00)	1.50 (1.00–4.00)		
	$t_{1/2z}$, h	Mean (SD)	7.79 (1.68)	10.0 (2.3)		
	V_z/F, L	Mean (SD)	1040 (573)	800 (425)		
	CL/F, L/h	Mean (SD)	98.0 (56.1)	59.0 (35.7)		
M1-1	C_{max}, ng/mL	GMean (CV%)	126 (39.0)	113 (30.9)	89.6	76.7–104.8
	AUC_{0-t}, μg·h/mL	GMean (CV%)	1.95 (44.9)	3.07 (38.1)	157.8	132.9–187.4
	$AUC_{0-\infty}$, μg·h/mL	GMean (CV%)	2.03 (42.5)	3.26 (39.4)	160.3	134.8–190.6
	T_{max}, h	Median (range)	3.50 (1.50–8.00)	4.00 (1.50–8.00)		
	$t_{1/2z}$, h	Mean (SD)	10.2 (3.2)	14.8 (4.6)		
M1-2	C_{max}, ng/mL	GMean (CV%)	41.8 (31.9)	59.2 (27.9)	141.7	123.0–163.2
	AUC_{0-t}, μg·h/mL	GMean (CV%)	0.700 (40.2)	1.48 (43.5)	210.7	177.6–250.1
	$AUC_{0-\infty}$, μg·h/mL	GMean (CV%)	0.751 (36.5)	1.54 (46.3)	204.3	173.5–240.6
	T_{max}, h	Median (range)	3.00 (1.00–4.00)	4.00 (3.00–8.00)		
	$t_{1/2z}$, h	Mean (SD)	11.3 (3.0)	13.3 (3.8)		
M1-6	C_{max}, ng/mL	GMean (CV%)	28.2 (43.0)	31.6 (31.3)	112.0	92.6–135.5
	AUC_{0-t}, μg·h/mL	GMean (CV%)	0.874 (44.1)	1.27 (41.3)	145.7	122.1–173.8
	$AUC_{0-\infty}$, μg·h/mL	GMean (CV%)	0.898 (43.0)[a]	1.25 (38.7)[b]	149.1[b]	123.9–179.6
	T_{max}, h	Median (range)	4.00 (3.00–24.0)	8.00 (3.00–24.0)		
	$t_{1/2z}$, h	Mean (SD)	16.1 (7.1)[a]	15.3 (4.5)[b]		
M9-2	C_{max}, ng/mL	GMean (CV%)	531 (36.2)	518 (31.7)	97.5	84.0–113.1
	AUC_{0-t}, μg·h/mL	GMean (CV%)	13.3 (41.5)	17.0 (32.6)	127.8	107.8–151.4
	$AUC_{0-\infty}$, μg·h/mL	GMean (CV%)	13.4 (41.5)	17.8 (34.6)	132.9	111.3–158.7
	T_{max}, h	Median (range)	6.00 (4.00–12.0)	8.00 (4.00–12.0)		
	$t_{1/2z}$, h	Mean (SD)	9.50 (1.82)	14.9 (4.7)		

C_{max}, maximum observed concentration; AUC_{0-t}, area under the concentration–time curve from time zero to the last measurable concentration; $AUC_{0-\infty}$, area under the concentration–time curve from time zero to infinity; T_{max}, time of the maximum concentration; $t_{1/2z}$, apparent terminal elimination half-life; V_z/F, apparent volume of distribution; CL/F, apparent clearance; GMean, geometric mean; CV, coefficient of variation; mean, arithmetic mean; SD, standard deviation; CI, confidence interval.

[a]Only 18 healthy volunteers had evaluable area under the concentration–time curve from zero to infinity and apparent terminal elimination half-life.

[b]Only 15 healthy volunteers had evaluable area under the concentration–time curve from zero to infinity and apparent terminal elimination half-life.

administered for 4 days prior to giving the apatinib dose and was continued throughout the apatinib PK sampling period to maintain enzyme inhibition. Compared with 100 mg itraconazole, the risk of severe adverse events for apatinib in healthy volunteers should be higher when coadministered with 200 mg itraconazole. However, using 100 mg once daily itraconazole could not attain maximize CYP3A inhibition to present the worst-case DDI scenario, which may result in underestimate of apatinib AUC ratio.

When apatinib is coadministered with itraconazole, it is nonequivalent. In the presence of itraconazole, C_{max}, AUC_{0-t}, and $t_{1/2z}$ of apatinib were all increased compared with those when apatinib was administered alone. The AUC_{0-t} of apatinib increased by approximately 75%, which might be because of the change in the bioavailability coupled with a reduction in the clearance of apatinib.

Although rifampin significantly reduced the AUC_{0-t} of apatinib as a result of enzyme induction, itraconazole produced a relatively minor effect on its coadministration with apatinib compared with its known effects on other CYP3A substrates. In vitro studies confirmed that CYP3A4 is the main enzyme involved in the metabolism of apatinib. The low ratio of AUC in the presence and absence of inhibitor is attributed to 4 factors: the multiple enzymes involved in the metabolism, the high K_m value, the low ratio of hepatic inhibitor concentration to K_i value, and the low hepatic extraction.[22] The metabolism of apatinib was catalyzed by multiple enzymes, thereby reducing the effect of CYP3A inhibitors. In addition, the K_m values associated with CYP3A4 were 0.57, 0.90, and 1.02 μmol/L for the formation of M1-1, M1-2, and M1-6, respectively.[6] These K_m values are approximately 180, 280, and 320 times greater than the apatinib

C_{max} observed in patients from study 2. None of the metabolizing enzymes were saturated when the plasma levels were lower than the K_m values. Another reason could be the dose of itraconazole that we used. A dose of 100 and 200 mg itraconazole orally once daily for 4 days increased the AUC of lovastatin by 15.4-fold and more than 20-fold, respectively.[23,24] A higher does of itraconazole probably would have led to a more pronounced interaction. The AUC_{0-t} values of M1-1, M1-2, M1-6, and M9-2 were increased by 58%, 111%, 46%, and 28%, respectively. In vitro studies indicated that M1-1, M1-2, and M1-6 are CYP3A4, P-gp, and BCRP substrates. Itraconazole is an inhibitor of CYP3A, P-gp, and BCRP.[25,26] Itraconazole may also have inhibited the metabolism and excretion of M1-1, M1-2, and M1-6, thereby increasing their exposure. Given that M9-2 is the *O*-glucuronide conjugate of M1-1, the exposure of M9-2 increases with that of M1-1.

Conclusions

In summary, the present study provides a detailed understanding of the PK drug interaction potential of apatinib. Coadministration of apatinib with strong inducers of CYP3A4 and strong inhibitors of CYP3A may decrease and increase the apatinib plasma concentration, respectively. A strong CYP3A4 inducer (rifampin) had a strong effect (>5-fold) on the clinical pharmacokinetics of apatinib, whereas a strong CYP3A inhibitor (itraconazole, 100 mg once daily) had a weak effect (1.25- to 2-fold). Whether these effects are of clinical significance needs further research and information about the exposure–safety and exposure–efficacy relationship of apatinib.

Declaration of Conflicting Interests

The authors declare no conflicts of interest that are directly relevant to the content of this study.

Funding

The study was supported by the National Natural Science Foundation of China (grant number 81521005).

References

1. Hu XC, Zhang J, Xu BH, et al. Multicenter phase II study of apatinib, a novel VEGFR inhibitor in heavily pretreated patients with metastatic triple-negative breast cancer. *Int J Cancer*. 2014;135(8):1961–1969.
2. Zhang HH, Chen FF, Wang ZQ, Wu SX. Successful treatment with apatinib for refractory recurrent malignant gliomas: a case series. *Onco Targets Ther*. 2017;10:837–845.
3. Deng LH, Wang Y, Lu WB, Liu Q, Wu J, Jin JH. Apatinib treatment combined with chemotherapy for advanced epithelial ovarian cancer: a case report. *Onco Targets Ther*. 2017;10:1521–1525.
4. Public summary of opinion on orphan designation N-(4-(1-cyanocyclopentyl)phenyl)-2-(4-pyridinylmethyl)amino-3-pyridinecarboxamide methanesulfonate for the treatment of gastric cancer. European Medicines Agency. http://www.ema.europa.eu/docs/en_GB/document_library/Orphan_designation/2017/03/WC500224877.pdf. Accessed June 2, 2017.
5. Yu MM, Gao ZW, Dai XJ, et al. Population pharmacokinetic and covariate analysis of apatinib, an oral tyrosine kinase inhibitor, in healthy volunteers and patients with solid tumors. *Clin Pharmacokinet*. 2017;56(1):65–76.
6. Ding JF, Chen XY, Gao ZW, et al. Metabolism and pharmacokinetics of novel selective vascular endothelial growth factor receptor-2 inhibitor apatinib in humans. *Drug Metab Dispos*. 2013;41(6):1195–1210.
7. Ding JF, Chen XY, Dai XJ, Zhong DF. Simultaneous determination of apatinib and its four major metabolites in human plasma using liquid chromatography-tandem mass spectrometry and its application to a pharmacokinetic study. *J Chromatogr B Analyt Technol Biomed Life Sci*. 2012;895-896:108–115.
8. Niemi M, Backman JT, Fromm MF, Neuvonen PJ, Kivistö KT. Pharmacokinetic interactions with rifampicin. *Clin Pharmacokinet*. 2003;42(9):819–850.
9. Chen JZ, Raymond K. Roles of rifampicin in drug-drug interactions underlying molecular mechanisms involving the nuclear pregnane X receptor. *Ann Clin Microbiol Antimicrob*. 2006;5:3.
10. US Food and Drug Administration: Center for Drug Evaluation and Research (CDER). Guidance for Industry: in vivo drug metabolism/drug interaction studies—study design, data analysis, implications for dosing, and labeling recommendations. 2012.
11. Bolton AE, Peng B, Hubert M, et al. Effect of rifampicin on the pharmacokinetics imatinib mesylate (Gleevec, STI571) in healthy subjects. *Cancer Chemother Pharmacol*. 2004;53(2):102–106.
12. Tanaka C, Yin OQ, Smith T, et al. Effects of rifampin and ketoconazole on the pharmacokinetics of nilotinib in healthy participants. *J Clin Pharmacol*. 2011;51(1):75–83.
13. SPRYCEL (dasatinib) tablets. US Prescribing Information. Bristol-Myers Squibb, Inc; September 2016.
14. Swaisland HC, Ranson M, Smith DA, et al. Pharmacokinetic drug interactions of gefitinib with rifampicin itraconazole and metoprolol. *Clin Pharmacokinet*. 2005;44(10):1067–1081.
15. Rakhit A, Pantze MP, Fettner S, et al. The effects of CYP3A4 inhibition on erlotinib pharmacokinetics: computer-based simulation (SimCYP) predicts in vivo metabolic inhibition. *Eur J Clin Pharmacol*. 2008;64(1):31–41.
16. Ohnhaus EE, Breckenridge AM, Park BK. Urinary excretion of 6β-hydroxycortisol and the time course measurement of enzyme induction in man. *Eur J Clin Pharmacol*. 1989;36(1):39–46.
17. Yoshizato T, Kotegawa T, Imai H, et al. Itraconazole and domperidone: a placebo-controlled drug interaction study. *Eur J Clin Pharmacol*. 2012;68(9):1287–1294.
18. Kantola T, Kivistö KT, Neuvonen PJ. Effect of itraconazole on the pharmacokinetics of atorvastatin. *Clin Pharmacol Ther*. 1998;64(1):58–65.
19. Jalava KM, Olkkola KT, Neuvonen PJ. Itraconazole greatly increases plasma concentrations and effects of felodipine. *Clin Pharmacol Ther*. 1997;61(4):410–415.
20. Ke AB, Zamek-Gliszczynski MJ, Higgins JW, Hall SD. Itraconazole and clarithromycin as ketoconazole alternatives for clinical CYP3A inhibition studies. *Clin Pharmacol Ther*. 2014;95(5):473–476.
21. Liu LC, Bello A, Dresser MJ, et al. Best practices for the use of itraconazole as a replacement for ketoconazole in drug-drug interaction studies. *J Clin Pharmacol*. 2016;56(2):143–151.

22. Pang XY, Zhang YF, Gao RN, Zhong K, Zhong DF, Chen XY. Effects of rifampin and ketoconazole on pharmacokinetics of morinidazole in healthy chinese subjects. *Antimicrob Agents Chemother*. 2014;58(10):5987–5993.
23. Kivistö KT, Kantola T, Neuvonen PJ. Different effects of itraconazole on the pharmacokinetics of fluvastatin and lovastatin. *Br J Clin Pharmacol*. 1998;46(1):49–53.
24. Neuvonen PJ, Jalava KM. Itraconazole drastically increases plasma concentrations of lovastatin and lovastatin acid. *Clin Pharmacol Ther*. 1996;60(1):54–61.
25. Vermeer LM, Isringhausen CD, Ogilvie BW, Buckley DB. Evaluation of ketoconazole and its alternative clinical CYP3A4/5 Inhibitors as inhibitors of drug transporters: the in vitro effects of ketoconazole, ritonavir, clarithromycin, and itraconazole on 13 clinically-relevant drug transporters. *Drug Metab Dispos*. 2016;44(3):453–459.
26. Lempers VJ, van den Heuvel JJ, Russel FG, et al. Inhibitory potential of antifungal drugs on ATP-binding cassette transporters P-glycoprotein, MRP1 to MRP5, BCRP, and BSEP. *Antimicrob Agents Chemother*. 2016;60(6):3372–3379.